FORMULATION, COMPUTATION AND APPLICATION OF OPTIMAL MEMBRANE TRIANGLE ELEMENT WITH DRILLING DEGREES OF FREEDOM

M. Paknahad[1], J. Noorzaei[1], M.S. Jaafar[1] and W. A. Thanoon[2]

[1]Department of Civil Engineering, Faculty of Engineering, Universiti Putra Malaysia, Serdang, Malaysia
[2]Department of Civil Engineering, Petronas University of Technology, Perak, Malaysia
Email: jamal@eng.upm.edu.my

ABSTRACT

In this study an alternate formulation (optimum membrane triangle (OPT) element that is to reduce the computer programming and the computational cost is presented. The accuracy of finite element program has been established by analyzing some standard benchmarks example. The numerical study indicate that using OPT element for a wide range of aspect ratio, shows the performance with good accuracy in finite element idealization with coarse mesh for analysis of a shear wall structure.

KEYWORDS: finite elements, high performance element, drilling freedoms, shear wall structure, assumed natural deviatoric strains.

INTRODUCTION

Since the evolution of the finite element, there have been significant developments in finite element methods. A large number of different finite elements have been developed and the finite element methods have been used for solving problems in different fields of engineering. The finite element methods became even more popular with the advancement of microcomputers and development of various efficient programming languages.

The refinement of the membrane element has gone about as far as it can go within the limitation of two degrees of freedom per node. Ever since 1967 element designers have considered the possibility of using the component of rotation normal to the plane of the element at its corner points as an additional nodal degree of freedom with which to improve the performance of three- and four-node membrane elements [1].

In-plane rotational degrees of freedom are referred to as "drilling degrees of freedom", as shown in Fig. 1. Drilling degrees of freedom are viewed as particularly displacement in plate and shell analysis.
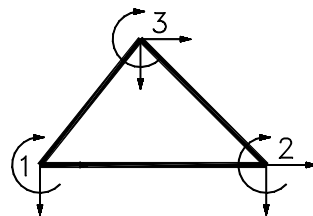

Figure 1: Membrane element with drilling degree of freedom

The idea of including normal-rotation degrees of freedom at corner points of plane-stress finite elements (the so-called drilling freedoms) is an old one [2-5]. The main objectives behind this idea are:

(a) To improve the element performance while avoiding the use of midpoint degrees of freedom. Midpoint nodes have lower valency than corner nodes, demand extra effort in mesh definition and generation, and can cause modeling difficulties in nonlinear analysis and dynamics.
(b) To solve the "normal rotation problem" of smooth shells analyzed with finite elements programs that carry six degrees of freedom per node.
(c) To simplify the modeling of connections between plates, shells and beams.

Sze, et al. [6] developed a mixed quadrilateral plane element with drilling degrees of freedom using Allman's interpolation scheme. Piancastelli [7] introduced a plate-type finite element with six degrees of freedom (DOF) for each node. Hughes et al. [5] investigated variational principles employing independent rotation fields. In the two-dimensional case these lead to membrane elements with "drilling degrees of freedom". Cook [8] developed a 24 degree of freedom quadrilateral shell element with drilling degree of freedom. He concluded that numerical results are good but the element is not the best available four-node shell element in all test cases.

Chinosi [9, 10] considered the membrane elements with drilling degrees of freedom and implemented a new finite element scheme with drilling degrees of freedom for linear elasticity problems and to show its convergence properties. Zhu, et al. [11] discussed the development of a new four-node general element with single point quadrature used for the analysis of non-linear geometrical and material problems. One of the main features of that element is the implementation of a rotation component. Lee, et al. [12] studied the analysis of folded structures and box beams by using drilling degree of freedom. The results obtained are in good agreement with the semi analytical solutions and numerical results reported by other investigators. Pimpinelli [13] studied a four nodes quadrilateral membrane with drilling degrees of freedom. The proposed numerical model is based on the minimization of the modified Hu–Washizu functional where the enhanced strain and the enhanced rotation fields are included. The stability and the convergence of the numerical method are discussed and the numerical examples show that the proposed finite element exhibits good behavior for distorted coarse mesh under bending stress states.

Ibrahimbegovic [14] presented a membrane element with drilling degrees of freedom based on a variational formulation which employs an independent rotation field. New membrane elements namely MQ2 and MQ3 are by Ibrahimbegovic [15] presented with rotational degrees of freedom. Both membrane elements are based on a variational foundation and both exhibit good performance over a set of problems. Furthermore, the Ibrahimbegovic [16,17,18] constructed a two-dimensional membrane element with drilling rotations for geometrically nonlinear elasticity with applying the mixed finite element method. In very extensive investigation   presented a consistent theoretical framework for a stress resultant geometrically nonlinear shell theory and discussed details of the numerical implementation of the geometrically nonlinear shell theory with drilling degree of freedom.

Felippa et al. [19,20] studied the formulation of 3-node, 9-dof membrane elements with normal-to-element-plane rotations (the so-called drilling freedoms) within the context of parameterized variational principles. They constructed an element of this type using the extended free formulation EFF and they constructed this element within the context of the assumed natural deviatoric strain (ANDES) formulation. The resulting formulation has five free parameters. These parameters are optimized against pure bending by energy balance methods. The performance of the resulting element is evaluated. Furthermore, Felippa [21] in an extensive report compare derivation methods for constructing optimal membrane triangles with corner drilling freedoms. The term "optimal" is used in the sense of exact inplane pure-bending response of rectangular mesh units of arbitrary aspect ratio. In this paper a comparative summary of element formulation approaches, the construction of an optimal 3-node triangle (OPT) using the ANDES formulation is presented.

The present investigation has been focused on following:

(i)   Formulation of triangle optimal element in a simple form, which makes the OPT element attractive as far as its programming and computational cost are concerned. The formulation is mainly based on the work of Felippa et al [19-21].
(ii)   Development and validation of a computer program based on (i).
(iii)   Applying the developed computer code in analysis of shear wall structures.

FORMULATION OF OPTIMAL MEMBRANE ELEMENTS

The Assumed Natural Deviatoric Strain (ANDES) formulation is a combination of the free formulation (FF) of Bergan and a variant of the Assumed Natural Strain (ANS) method according to Park et al. [22]. Extensive formulation of ANS and ANDES published in work of Felippa et al. [19-21]. The basic steps of formulation are summarized in below. The narrative assumes that the element to be constructed has nodal displacement degrees of freedom collected in vector v, elastic modulus matrix E, and volume V. ANDES is a variant of ANS that exploits the fundamental decomposition of the stiffness equations:

$$K v = (K_b + \alpha K_h) \, v = p \tag{1}$$

Here K_b is the basic stiffness, which takes care of consistency, and K_h is the higher order stiffness, which takes care of stability (rank sufficiency) and accuracy. This decomposition was found by Bergan [23] as part of the Free Formulation (FF) and $\alpha > 0$ is a scaling coefficient. The basic stiffness matrix K_b is constructed by the standard procedure (CST element). The mean portion of the strains is left to be determined variationally from the constant stress assumptions used to develop K_h.

Element Description
The membrane triangle shown in Fig. 2 has straight sides joining the corners defined by the coordinates $\{x_i , y_i\}$, $i = 1, 2, 3$. Coordinate differences are abbreviated $x_{ij} = x_i - x_j$ and $y_{ij} = y_i - y_j$. The signed area A is given by
$$2A = (x_2 y_3 - x_3 y_2) + (x_3 y_1 - x_1 y_3) + (x_1 y_2 - x_2 y_1) = y_{21}x_{13} - x_{21}y_{13}$$
In addition the l_{ij}'s are the lengths of the sides. The triangle will be assumed to have constant thickness h and uniform plane stress constitutive properties.

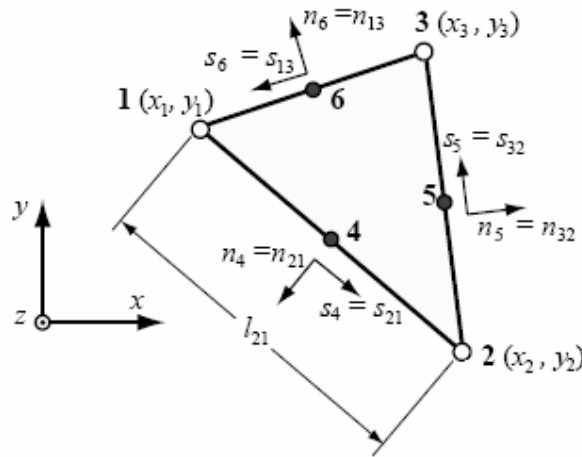$$l_{ij} = l_{ji} = \sqrt{x_{ij}^2 + y_{ij}^2} \tag{2}$$

Figure 2: Triangle geometry

The well known triangle coordinates are denoted by $\zeta1$, $\zeta2$ and $\zeta3$, which satisfy $\zeta1 + \zeta2 + \zeta3 = 1$. The degrees of freedom, are collected in the node displacement vector;

$$u_R = [u_{x1}\ u_{y1}\ \theta_1\ u_{x2}\ u_{y2}\ \theta_2\ u_{x3}\ u_{y3}\ \theta_3]^T \tag{3}$$

Here u_{xi} and u_{yi} denote the nodal values of the translational displacements u_x and u_y along x and y, respectively, and $\theta \equiv \theta_z$ are the "drilling rotations" about z (positive counter clockwise when looking down on the element midplane along -z).

Natural Strains
In the derivation of the higher order stiffness by ANDES [19] natural strains play a key role. Strains along the 3 side directions were used in [19]. The natural strains are collected in the 3-vector as showed in fig. 3: [21]

$$\varepsilon = \begin{bmatrix} \varepsilon_{21} & \varepsilon_{32} & \varepsilon_{13} \end{bmatrix}^T \tag{4}$$
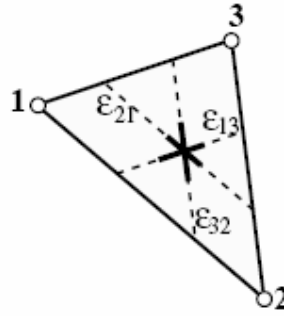
Figure 3: Natural strains, along side directions

The natural strains are related to Cartesian strains $\{e_{xx}, e_{yy}, 2e_{xy}\}$ by the "strain gage rosette" transformation. Strain gage rosette are given by;

$$\epsilon = \begin{bmatrix} \epsilon_{12} \\ \epsilon_{23} \\ \epsilon_{31} \end{bmatrix} = \begin{bmatrix} x_{21}^2/\ell_{21}^2 & y_{21}^2/\ell_{21}^2 & x_{21}y_{21}/\ell_{21}^2 \\ x_{32}^2/\ell_{32}^2 & y_{32}^2/\ell_{32}^2 & x_{32}y_{32}/\ell_{32}^2 \\ x_{13}^2/\ell_{13}^2 & y_{13}^2/\ell_{13}^2 & x_{13}y_{13}/\ell_{13}^2 \end{bmatrix} \begin{bmatrix} e_{xx} \\ e_{yy} \\ 2e_{xy} \end{bmatrix} = \mathbf{T}_e^{-1}\mathbf{e},$$

(5)

The inverse relationship in matrix notation is $e = \mathbf{T}_e \, \varepsilon$. The natural stress-strain matrix $\mathbf{E}_{nat}$ is defined by

$$\mathbf{E}_{nat} = \mathbf{T}_e^{T} \mathbf{E} \mathbf{T}_e$$

(6)

which is constant over the triangle [21].

The Basic Stiffness

An explicit form of the basic stiffness for the LST was obtained in 1984 and published the following year. It can be expressed as $\mathbf{K}_b = V^{-1} \mathbf{L} \mathbf{E} \mathbf{L}^{T}$. Where $V = Ah$ is the element volume, and $\mathbf{L}$ is a 3 × 9 matrix that contains a free parameter α_b: [19-21,23];

$$\mathbf{L} = \tfrac{1}{2}h \begin{bmatrix} y_{23} & 0 & x_{32} \\ 0 & x_{32} & y_{23} \\ \tfrac{1}{6}\alpha_b y_{23}(y_{13}-y_{21}) & \tfrac{1}{6}\alpha_b x_{32}(x_{31}-x_{12}) & \tfrac{1}{3}\alpha_b(x_{31}y_{13}-x_{12}y_{21}) \\ y_{31} & 0 & x_{13} \\ 0 & x_{13} & y_{31} \\ \tfrac{1}{6}\alpha_b y_{31}(y_{21}-y_{32}) & \tfrac{1}{6}\alpha_b x_{13}(x_{12}-x_{23}) & \tfrac{1}{3}\alpha_b(x_{12}y_{21}-x_{23}y_{32}) \\ y_{12} & 0 & x_{21} \\ 0 & x_{21} & y_{12} \\ \tfrac{1}{6}\alpha_b y_{12}(y_{32}-y_{13}) & \tfrac{1}{6}\alpha_b x_{21}(x_{23}-x_{31}) & \tfrac{1}{3}\alpha_b(x_{23}y_{32}-x_{31}y_{13}) \end{bmatrix}.$$

(7)

In the FF this is called a force-lumping matrix, If $\alpha_b = 0$ the basic stiffness reduces to the total stiffness matrix of the CST element, in which case the rows and columns associated with the drilling rotations vanish. In the direct fabrication approach the decomposition is explicitly used in the two-stage construction of the element: first K_b and then K_h.

The Higher Order Stiffness

The ANDES form of higher order stiffness matrix $\mathbf{K}_h$ developed in [19], is

$$\mathbf{K}_h = c_{fac} \tilde{\mathbf{T}}_{\theta u}^{T} \mathbf{K}_\theta \tilde{\mathbf{T}}_{\theta u}.$$

(8)

Where K_θ is the 3 × 3 higher order stiffness in terms of the hierarchical rotations $\tilde{\theta}$ and c_{fac} is a scaling factor [21]. To express $\mathbf{K}_\theta$ compactly, introduce the following matrices, which depend on nine free dimensionless parameters, $\beta1$ through $\beta9$:

$$\mathbf{Q}_1 = \frac{2A}{3}\begin{bmatrix} \frac{\beta_1}{\ell_{21}^2} & \frac{\beta_2}{\ell_{21}^2} & \frac{\beta_3}{\ell_{21}^2} \\ \frac{\beta_4}{\ell_{32}^2} & \frac{\beta_5}{\ell_{32}^2} & \frac{\beta_6}{\ell_{32}^2} \\ \frac{\beta_7}{\ell_{13}^2} & \frac{\beta_8}{\ell_{13}^2} & \frac{\beta_9}{\ell_{13}^2} \end{bmatrix}, \quad \mathbf{Q}_2 = \frac{2A}{3}\begin{bmatrix} \frac{\beta_9}{\ell_{21}^2} & \frac{\beta_7}{\ell_{21}^2} & \frac{\beta_8}{\ell_{21}^2} \\ \frac{\beta_3}{\ell_{32}^2} & \frac{\beta_1}{\ell_{32}^2} & \frac{\beta_2}{\ell_{32}^2} \\ \frac{\beta_6}{\ell_{13}^2} & \frac{\beta_4}{\ell_{13}^2} & \frac{\beta_5}{\ell_{13}^2} \end{bmatrix}, \quad \mathbf{Q}_3 = \frac{2A}{3}\begin{bmatrix} \frac{\beta_5}{\ell_{21}^2} & \frac{\beta_6}{\ell_{21}^2} & \frac{\beta_4}{\ell_{21}^2} \\ \frac{\beta_8}{\ell_{32}^2} & \frac{\beta_9}{\ell_{32}^2} & \frac{\beta_7}{\ell_{32}^2} \\ \frac{\beta_2}{\ell_{13}^2} & \frac{\beta_3}{\ell_{13}^2} & \frac{\beta_1}{\ell_{13}^2} \end{bmatrix}$$

(9)

Matrix $\mathbf{Q}_i$ relates the natural strains i at corner i to the deviatoric corner curvatures $\tilde{\theta}$. Evaluate at the midpoints:

$$\mathbf{Q}_4 = \tfrac{1}{2}(\mathbf{Q}_1 + \mathbf{Q}_2), \quad \mathbf{Q}_5 = \tfrac{1}{2}(\mathbf{Q}_2 + \mathbf{Q}_3), \quad \mathbf{Q}_6 = \tfrac{1}{2}(\mathbf{Q}_3 + \mathbf{Q}_1)$$

$$\mathbf{K}_\theta = h\left(\mathbf{Q}_4^T \mathbf{E}_{nat}\mathbf{Q}_4 + \mathbf{Q}_5^T \mathbf{E}_{nat}\mathbf{Q}_5 + \mathbf{Q}_6^T \mathbf{E}_{nat}\mathbf{Q}_6\right),$$

$$\mathbf{K}_h = \tfrac{3}{4}\beta_0 \mathbf{T}_{\theta u}^T \mathbf{K}_\theta \mathbf{T}_{\theta u}$$

(10)

where β_0 is an overall scaling coefficient. So finally K_R assumes a template form with 11 free parameters: $\alpha_b, \beta_0, \beta_1, \dots \beta_9$: [21]

$$\mathbf{K}_R(\alpha_b, \beta_0, \beta_1, \dots \beta_9) = V^{-1}\mathbf{LEL}^T + \tfrac{3}{4}\beta \tilde{\mathbf{T}}_{\theta u}^T \mathbf{K}_\theta \tilde{\mathbf{T}}_{\theta u}.$$

(11)

The free dimensionless parameters are determined from a higher order patch test which tunes up the higher order stiffness of triangular elements. Using such a patch test the optimal parameters are calculated and tabulated in Table 1 [21]:

Table 1: Dimensionless parameter of OPT element

αb	β0	β1	β2	β3	β4	β5	β6	β7	β8	β9
3/2	1/2	1	2	1	0	1	−1	−1	−1	−2

FAST CALCULATION OF HIGHER ORDER STIFFNESS MATRIX

In this study an alternative formulation of the above element is presented which is more efficient compare to the optimal element constructed by Felippa [21]. The programming aspect and implementation the element is a simple task. In the subsequent discussion these formulation are brought in details. Let assume LL matrix as:

$$LL = \begin{bmatrix} l_{21}^2 & 0 & 0 \\ 0 & l_{32}^2 & 0 \\ 0 & 0 & l_{13}^2 \end{bmatrix}$$

(12)

With assuming this matrix we can rewrite the formulation of Q_i and T_e as:

$$Q_i = LL^{-1}Q_i^* \qquad T_e = T_e^* LL \quad \text{and} \quad E_{nat}^* = T_e^{*T} E\, T_e^*$$

(13)

Where:

$$Q_1^* = \frac{2A}{3}\begin{bmatrix} \beta_1 & \beta_2 & \beta_3 \\ \beta_4 & \beta_5 & \beta_6 \\ \beta_7 & \beta_8 & \beta_9 \end{bmatrix} \quad Q_2^* = \frac{2A}{3}\begin{bmatrix} \beta_9 & \beta_7 & \beta_8 \\ \beta_3 & \beta_1 & \beta_2 \\ \beta_6 & \beta_4 & \beta_5 \end{bmatrix} \quad Q_3^* = \frac{2A}{3}\begin{bmatrix} \beta_5 & \beta_6 & \beta_4 \\ \beta_8 & \beta_9 & \beta_7 \\ \beta_2 & \beta_3 & \beta_1 \end{bmatrix}$$

(14)

It can be written:

$$Q_4^* = LL^{-1}Q_4 \qquad Q_5^* = LL^{-1}Q_5 \qquad Q_6^* = LL^{-1}Q_6$$

(15)

With substituting our new form of T_e and Q_i in high order stiffness formulation and expanding it we can write:

$$K_\theta = h(Q_4^{*T} E_{nat}^* Q_4^* + Q_5^{*T} E_{nat}^* Q_5^* + Q_6^{*T} E_{nat}^* Q_6^*) \ldots$$

(16)

Hence the formulation of K_h with new notation is more efficient in view point of computational time and effort compare to that of Felippa [21]. Also same formulation adapted for calculation of stresses.

FINITE ELEMENT PROGRAM

The existing two dimensional finite element analysis program written by Noorzaei et al.[24] has been extensively modified in view of inclusion of optimal ANDES element which is based on new formulation present in this paper[25]. The program element library includes several conventional finite element such as beam, truss, Finite and Infinite 2-D Isoparametric element. This program is multi element, multi degrees of freedom and dynamically dimensioned features. The program is written in FORTRAN language and works under FORTRAN power station environment.

TESTING AND VERIFICATION

In order to validate the formulation, computational algorithm and implementation of new formulation of ANDES element, two benchmark examples available in the literature are presented. [19] Table 2 shows the notations used for previous results in literature.

Table 2: Identifier of Triangle Element Instances

Name	Description
ALL-3I	Allman 88 element integrated by 3-point interior rule.
ALL-3M	Allman 88 element integrated by 3-midpoint rule.
ALL-LS	Allman 88 element, least-square strain fit.
CST	Constant strain triangle CST-3/6C.
LST-Ret	Retrofitted LST with $\alpha b = 4/3$.
OPT	Optimal ANDES Template.

Example 1- Cantilever beam under End Moment

The slender cantilever beam of Fig. 4 is subjected to an end moment $M = 100$. The exact tip deflection $\delta_{tip} = ML/(2EI)$ is 100. The geometric data, material properties, boundary condition, loading and dimension of the beam are also presented in the figure.
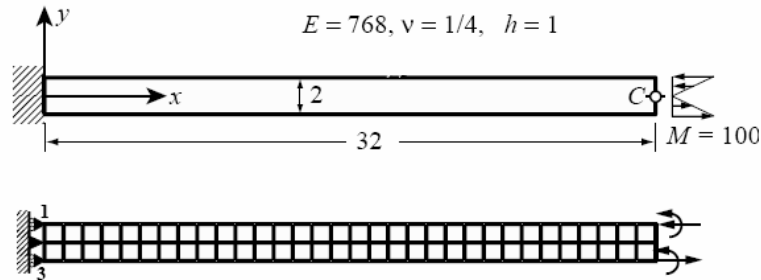
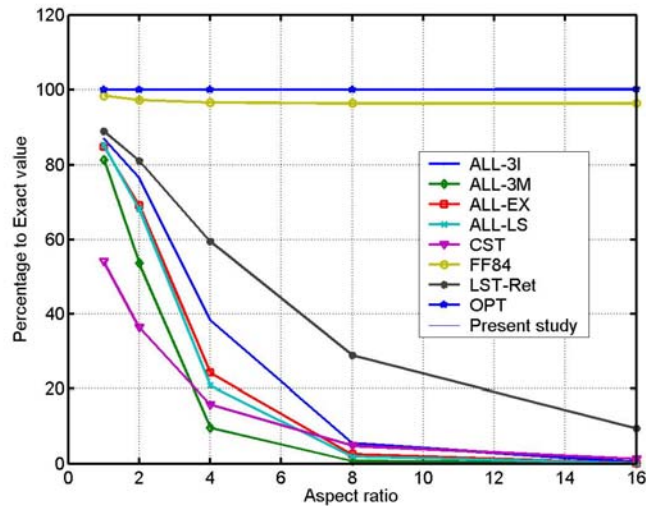*Figure 4: Slender cantilever beam under end moment*

Figure 5: Tip deflection for cantilever beam (exact=100)

The above example has been discretized regular meshes ranging from 2×2 to 32×2 , each rectangle mesh unit being composed of four half-thickness overlaid triangles. The element aspect ratios vary from 1:1 through 16:1. Fig. 5 shows computed tip deflections for several element types and five aspect ratios (1, 2, 4, 8, and 16) respectively. It is clear from this plot that there is a good agreement between the results evaluated from the present study and that reported in the literature. Moreover the FF84 element maintains good but not perfect accuracy. The Allman 88 triangle performs well for unit aspect ratios but rapidly becomes over stiff for $\gamma > 2$.

Example 2- The Shear-Loaded Short Cantilever
The shear-loaded cantilever beam defined in Fig. 6 has been selected as a test problem for plane stress elements by many investigators since originally proposed in [20]. The geometrical data, material property, boundary condition and loading are exhibited in Fig. 6.
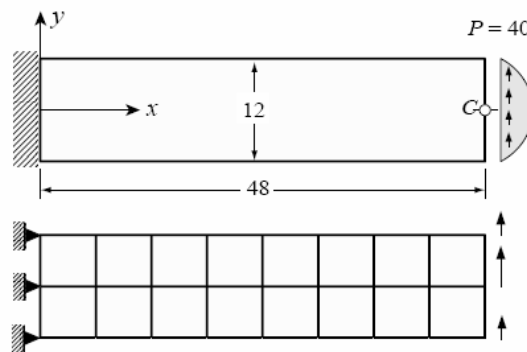

Figure 6: Cantilever under end shear: E = 30000, ν = 1/4, h = 1

The comparison value is the tip deflection δ_c at the center of the end-loaded cross section. An approximate solution derived from 2-D elasticity, based on a polynomial Airy stress function, gives δ_c = 0.34133+0.01400 = 0.35533, where the first term comes from the bending deflection, and the second from a *y*-quadratic shear field. Fig. 7 gives computed deflections for rectangular mesh units with aspect ratios of 1, 2 and 4 respectively. Mesh units consist of four half-thickness overlaid triangles. For reporting purposes the load was scaled so that the "theoretical solution" becomes 100.00. Of the four Allman triangle versions again ALL-3I outperformed the others. The results for FF84 and OPT triangles are very similar, without the latter displaying the clear advantages of Example 1. Prediction of result by present finite element program coincide with OPT element.
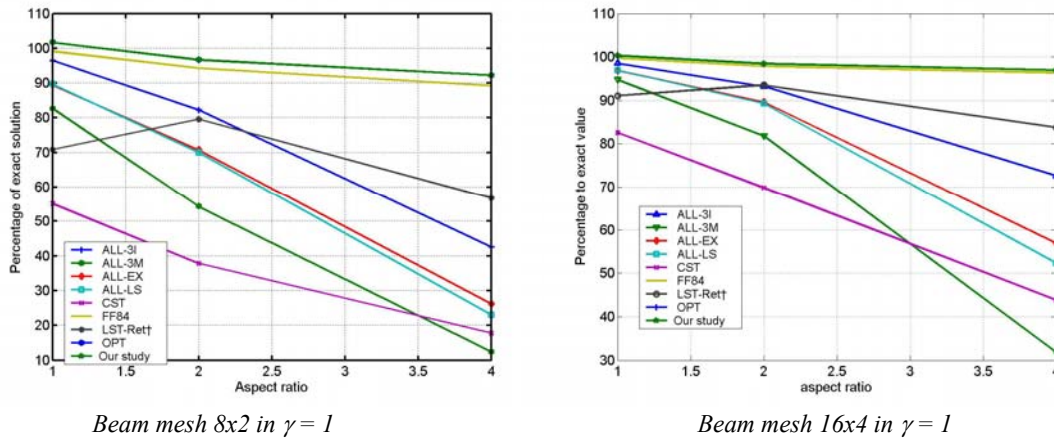

Beam mesh 8x2 in γ = 1 *Beam mesh 16x4 in γ = 1*

Figure 7: Tip deflection for short cantilever

APPLICATION OF OPTIMAL ELEMENT IN SHEAR WALL STRUCTURE

In order to show the efficiency, suitability, accuracy and superiority of the OPT element an attempt has been made to analyze the shear wall structure with opening employing the following commercial package namely SAP-2000, STAAD-PRO and Finite element program base on plane stress formulation. The structure was represented by two finite element models namely Model A (coarse mesh) and Model B (fine mesh) as depicted in Fig. 8.

The lateral displacement of each model at story 2, 4, 6 and 8 for all the all finite element codes has been tabulated in table 3. It is clear from this table OPT element gave the most suitable result as compared with the other commercial packages. It can be said that the shear wall structure can be analyzed using OPT element even having coarse mesh. Fig. 8 shows geometry and material property of an eight story coupled shear wall.
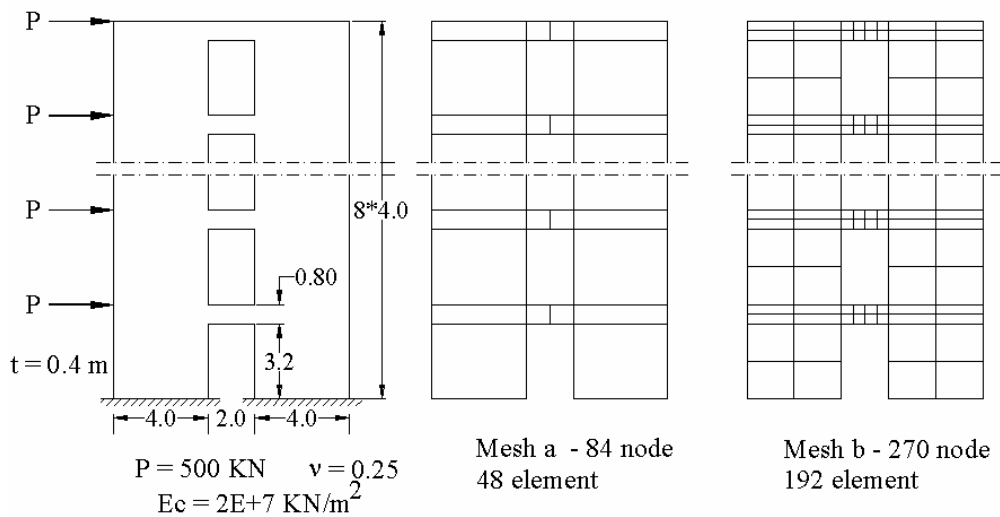

Mesh a - 84 node 48 element

Mesh b - 270 node 192 element

$P = 500\ KN$ $\nu = 0.25$
$Ec = 2E+7\ KN/m^2$

Figure 8: Geometry and material of coupled shear wall

Table 3: Comparison of the Lateral deflection at different story level

Finite element Method	Model	Lateral displacement at floor level			
		Floor 2	Floor 4	Floor 6	Floor 8
Finite element	Model a	0.56	1.53	2.59	3.62
	Model b	0.68	1.82	3.02	4.16
	Differentiate %	21.4	18.9	16.6	14.9
SAP2000	Model a	0.55	1.48	2.54	3.62
	Model b	0.77	2.06	3.40	4.66
	Differentiate %	40.0	39.1	33.8	35.5
STAAD-PRO	Model a	0.68	1.68	2.78	3.86
	Model b	0.79	2.08	3.44	4.69
	Differentiate %	16.1	23.8	23.7	21.5
OPT element	Model a	0.71	1.91	3.19	4.43
	Model b	0.74	1.98	3.28	4.51
	Differentiate %	4.2	3.6	2.82	1.8

Stress distribution

Contour of normal stress distribution, σ_x calculated by STAAD-PRO and SAP 2000 and present study are depicted in Figs. 9 and 10 respectively. It is seen from these plots that Finite element program using OPT element is capable to predict almost similar stress distribution in the shear wall as well as at the connecting beams. Moreover the stress distribution evaluated from the present study is from coarse finite element mesh in comparison with that of commercial packages with fine mesh.
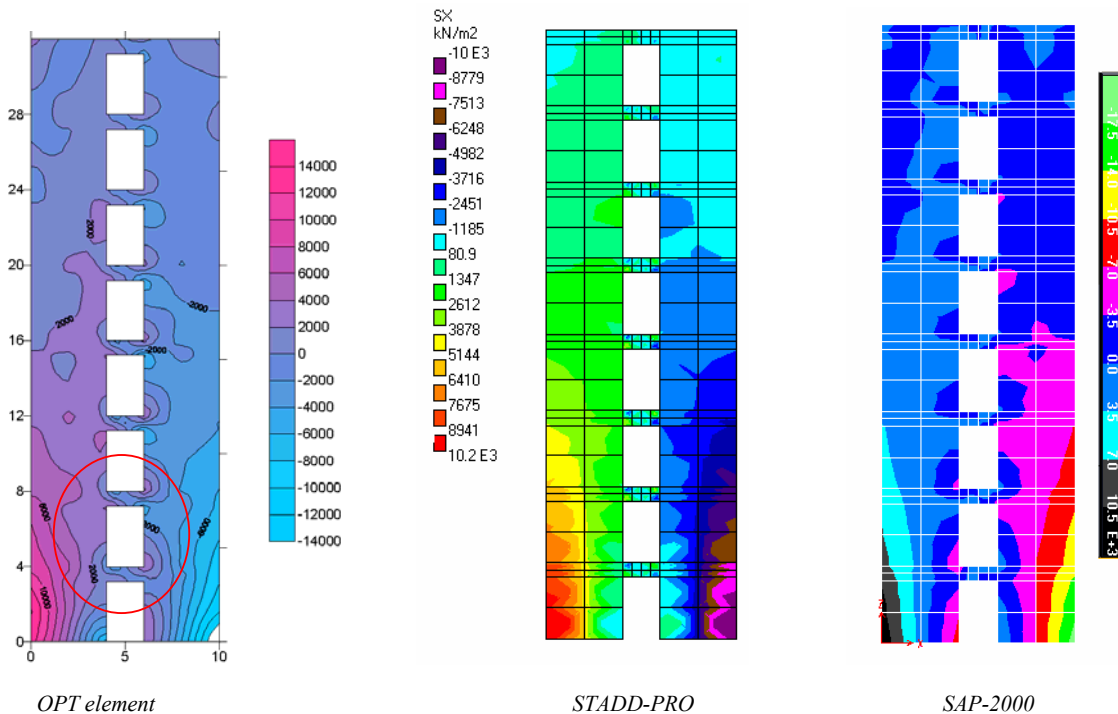

OPT element   *STADD-PRO*   *SAP-2000*

Figure 9: Contour of normal stress for shear wall
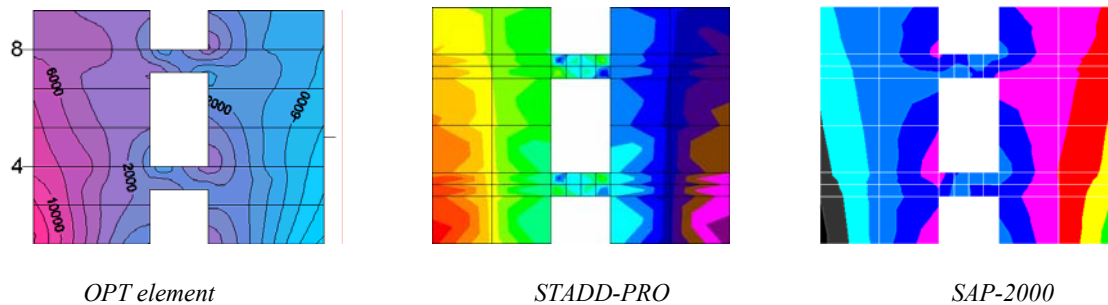
| *OPT element* | *STADD-PRO* | *SAP-2000* |

Figure 10: Contour of normal stress for connection beam

CONCLUSION

In this study an alternate formulation OPT elements, which reduce the computer programming and the computational cost, have been presented. The accuracy of finite element program has been established by analyzing some standard benchmarks example. The numerical study indicates that using OPT element for a wide range of aspect ratio, shows the performance of good accuracy in finite element idealization with coarse mesh for analysis of shear wall structure.

REFERENCES

[1]   G. M. Stanley, K. C. Park and T. J. R. Hughes, (1986), Continuum based resultant shell elements, in T. J. R. Hughes and E. Hinton (eds.), Finite Element Methods for Plate and Shell Structures, Vol. I: Element Technology, Pineridge Press, Swansea, U.K., (pp. 1-45)

[2]   J.L. Tocher and B.J. Hartz, (1967), "Higher order finite elements for plane stress", J. Eng. Mech. Div., Proc. ASCE 93 (EM4), (pp. 149-172)

[3]   M. K. Nygard, 1986, The Free Formulation for nonlinear finite elements with applications to shells, Ph. D. Disser-tation, Division of Structural Mechanics, NTH, Trondheim, Norway.

[4]   T. Belytschko, W. K. Liu and B. E. Engelmann, (1986), The gamma elements and related developments, in T. J. R. Hughes and E. Hinton (eds.), Finite Element Methods for Plate and Shell Structures, **1**: Element Technology, Pineridge Press, Swansea, U.K. (pp. 316–347).

[5]   T.J.R. Hughes, and F. Brezzi, (1989), On drilling degrees of freedom, Computer methods in applied mechanics and engineering, **72**: 105-121.

[6]   K. Y. Sze, C. Wanji and Y. K. Cheung, (1992), An efficient quadrilateral plane element with drilling degrees of freedom using orthogonal stress modes, Computers & Structures **42**(5): 695-705.

[7]   L. Piancastelli, (1992), Some considerations on a four –node finite element for composites with the drilling degrees of freedom, Computers & Structures **43**(2): 337-342.

[8]   R. D. Cook, (1994), Four node flat shell element, drilling degrees of freedom, membrane-bending coupling, warped geometry, and behavior, Computers & Structures **50**(4): 549-555.

[9]   C. Chinosi, (1995), Shell elements as a coupling of plate and drill elements, Computers & Structures **57**(5): 893-902.

[10] C. Chinosi, M.I. Comodi and G., Sacchib (1997), A new finite element with 'drilling' D.O.F., Comput. Methods Appl. Mech. Engrg. **143**: 1-11.

[11] Y. Zhu, and T. Zacharia, (1996), A new one-point quadrilateral, quadrilateral shell element with drilling degrees of freedom, Comput. Methods Appl. Mech. Engrg, **136**: 165-203.

[12] S.Y. Lee, and S.C. Wooh, (2004), Finite element vibration analysis of composite box structures using the high order plate theory, Journal of Sound and Vibration, **277**: 801–814.

[13] G. Pimpinelli, (2004), An assumed strain quadrilateral element with drilling degrees of freedom, Finite Elements in Analysis and Design **41**: 267–283.

[14] A. Ibrahimbegovic, (1990), A novel membrane finite element with an enhanced displacement interpolation, Finite Elements in Analysis and Design, **7**: 167-179.

[15] A. Ibrahimbegovic and F. Frey, (1992), membrane quadrilateral finite elements with rotational degrees of freedom, Engineering Fracture Mechanics **43**(1): 13-24.

[16] A. Ibrahimbegovic, (1993), Mixed finite element with drilling rotations for plane problems in finite elasticity, Computer Methods in Applied Mechanics and Engineering. **107**: 225-238.

[17] A. Ibrahimbegovic, (1994), Stress resultant geometrically nonlinear shell theory with drilling rotations-Part I. A consistent formulation, Comput. Methods Appl. Mech. Engrg. **118**: 265-284.

[18] A. Ibrahimbegovic, and F. Frey, (1994), Stress resultant geometrically nonlinear shell theory with drilling rotations-Part II. Computational aspects, Comput. Methods Appl. Mech. Engrg. **118**: 285-308.

[19] C. A. Felippa and C. Militello, (1992), Membrane triangles with corner drilling freedoms II. The ANDES element, Finite Elements in Analysis and Design **12**: 189-201.

[20] C. A. Felippa and S. Alexander, (1992), Membrane triangles with corner drilling freedoms III. Implementation and performance evaluation, Finite Elements in Analysis and Design, **12**: 203-239.

[21] C. A. Felippa, (2003), A Study of Optimal Membrane Triangles with Drilling Freedoms ,Department of Aerospace Engineering Sciences and Centre for Aerospace structures university of Colorado Boulder, Report CU-CAS-03-02.

[22] K. C. Park and G. M. Stanley, (1986), A curved C° shell element based on assumed natural-coordinate strains, J. Appl. Mech., **53**: 278-290.

[23] P. G. Bergan and C. A. Felippa, (1985), A triangular membrane element with rotational degrees of freedom, Comp. Meths. Appl. Mech. Engrg. **50**: 25–69.

[24]   J. Noorzaei, M.N. Viladkar and P.N. Godbole, (1995), Elasto-plastic analysis for soil structure interaction in framed structures, Computer and Structure. **55**(5): 797- 807.

[25] M.Paknahad '2D linear and nonlinear interaction analysis of shear wall building-foundation-soil system with static and seismic loading, PhD Thesis Department of Civil Engineering ,Universiti Putra Malaysia (in progress).